JOURNAL OF VIROLOGY, May 2003, p. 5152–5166 Vol. 77, No. 9
0022-538X/03/$08.00+0 DOI: 10.1128/JVI.77.9.5152–5166.2003

Functional Dissection of a Poliovirus *cis*-Acting Replication Element [PV-*cre*(2C)]: Analysis of Single- and Dual-*cre* Viral Genomes and Proteins That Bind Specifically to PV-*cre* RNA

Jiang Yin, Aniko V. Paul, Eckard Wimmer, and Elizabeth Rieder*

Department of Molecular Genetics and Microbiology, School of Medicine, State University of New York at Stony Brook, Stony Brook, New York 11794

Received 11 September 2002/Accepted 5 February 2003

The role of the *cis* replication element (*cre*) in the $2C^{ATPase}$ coding region of the poliovirus (PV) genome has been studied with a series of mutants derived from either a PV1 full-length genome or a replicon (P/L) containing the firefly luciferase reporter gene in place of the capsid region. Using the P/L replicon we have inserted *cre* elements at three different locations in the genome including the 5′ nontranslated region and within the open reading frame. The successful recovery of replication of a nonviable P/L (A_5C) mutant replicon with an artificial *cre* element as "rescuer," in addition to the results of site-directed mutagenesis and experiments with truncated forms of PV-*cre*(2C), indicated that (i) the sequence within the upper stem and loop regions contains the minimal *cre* RNA required for VPg uridylylation in vitro, (ii) the location of the *cre* RNA in the poliovirus genome is not relevant to RNA infectivity, and (iii) specific binding of $3CD^{pro}$ to PV-*cre*(2C) occurs within the upper stem region and probably involves several contact residues. The role of a 14-nucleotide conserved "core" sequence among known *cre* structures in picornaviruses was examined by site-directed mutagenesis of individual nucleotides. In addition to a conserved AAA (4472 to 4474) triplet previously shown to be the primary RNA template for VPg uridylylation by the PV RNA polymerase $3D^{pol}$ (E. Rieder, A. V. Paul, D. W. Kim, J. H. van Boom, and E. Wimmer, J. Virol. 74:10371-10380, 2000), we have now shown that important residues (G_{4468} and A_{4481}) are contained in a predicted internal bulge at the upper stem-loop of PV-*cre*(2C). We have further demonstrated that the viral proteins $3CD^{pro}$ and $3C^{pro}$ form stable complexes with a transcript PV-*cre*(2C) RNA that can be considered critical for VPg uridylylation.

The interplay of viral proteins and host factors in virus replication within the *Picornaviridae* has been the subject of studies for 2 decades. Although important discoveries emerged from these studies, the steps required to successfully replicate picornavirus RNA in host cells are not yet fully understood.

During the course of infection poliovirus RNA serves as mRNA and directs the synthesis of a large polyprotein, which is processed by virus-encoded proteinases into structural and nonstructural proteins. The genome of poliovirus possesses a 5′ end characteristic of picornaviruses, consisting of a long nontranslated region (5′ NTR) that is linked to a small viral peptide, VPg. The linkage is between the 5′ phosphate of the terminal UMP and the hydroxyl group of a tyrosine in VPg (2, 32). The 5′ NTR contains two highly structured RNA signals: the cloverleaf, which is required for genome replication (3, 4), and the internal ribosome entry site (IRES; (12, 28), which directs translation initiation (Fig. 1). The cloverleaf has been shown to interact with viral protein $3CD^{pro}$ and either 3AB or cellular poly(rC) binding protein (PCBP2) to perform its function in RNA synthesis (4, 6, 7, 10, 21, 31, 39). More recently, a model of the genome in a circular form aided by the interaction between CL, $3CD^{pro}$, and PCBP2 at the 5′ NTR and poly(A) and poly(A) binding protein on the 3′ NTR has been proposed (5, 11).

The poly(A) tail and the heteropolymeric region of the 3′ NTR (Fig. 1) contain signals for replication of the poliovirus genome. Despite the observed deleterious effects of mutations within the heteropolymeric region, the role of this highly structured segment of the poliovirus genome in virus replication remains unsolved (1). Truncated forms of the genome lacking the 3′ NTR have been shown to replicate, albeit not as efficiently as the wild-type genome (35).

A new structural element, *cre* (*c*is replication element, *ori*I), has been identified in the genomes of several picornaviruses. *cre*s have been described for human rhinovirus 14 (HRV14) (18), cardioviruses (Theiler's murine encephalomyelitis virus 15), poliovirus types 3 and 1 (9, 26, 30), HRV2 (8) (Fig. 2), and foot-and-mouth disease virus (17). Interestingly, the locations of these elements in the genomes of different picornaviruses vary, although all seem to perform the same function. In assays where the uridylylation partners are reconstituted from purified viral proteins, the *cre* elements act entirely independently of other RNA signals of the genomic RNA (26, 30) (E. Rieder et al., submitted for publication). This extends to a variant of poliovirus RNA, whose cloverleaf cannot bind $3CD^{pro}$ yet functions with wild-type (wt) efficiency in uridylylation (Rieder et al., submitted). In contrast, in studies of the translation/replication system reported by Lyons et al. (16), the cloverleaf was found to be essential for uridylylation of VPg. This appar-

* Corresponding author. Mailing address: Department of Molecular Genetics and Microbiology, School of Medicine, State University of New York at Stony Brook, Stony Brook, NY 11794. Phone: (631) 632-8804. Fax: (631) 632-8891. E-mail: ariederrojas@notes.cc.sunysb.edu.

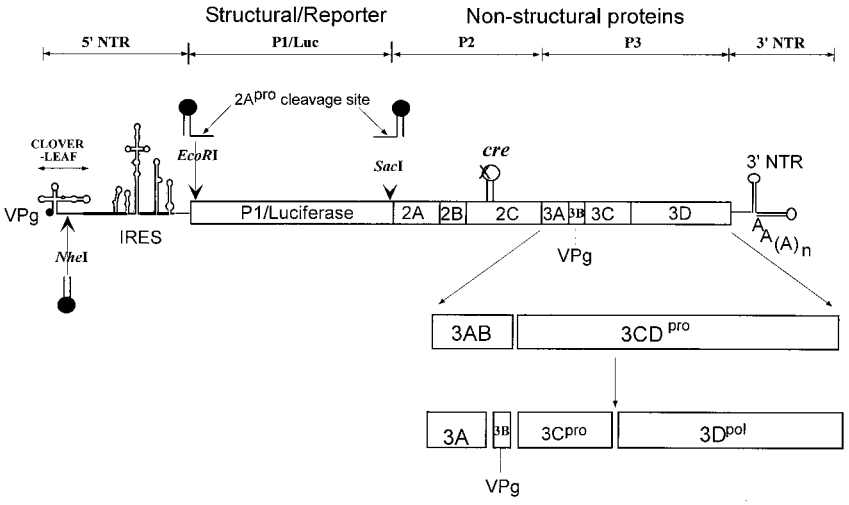

FIG. 1. Schematic diagram of replicon and full-length poliovirus genomes used in this study. Open circle, wt PV-*cre*(2C). Arrows, positions of unique restriction endonuclease sites engineered for the insertion of the second copy of *cre* of various origins. In rescue experiments, the native *cre*(2C) was inactivated through a point mutation (A_5C) in the conserved AAA sequence of the PV-*cre* loop (X) and a second copy of *cre* (filled hairpin loop) from poliovirus, HRV2, or HRV14 or an artificial *cre* was inserted at locations indicated by arrows.

ent conflict in the results remains to be resolved and may be due to differences in the experimental approach.

cre RNAs so far described for picornaviruses consist of a hairpin structure composed of a stem that is heterogeneous in length and that includes internal bulges and a terminal loop of variable size (Fig. 2). Recently, we have shown that poliovirus RNA containing a mutation (underlined) of AAA to CAA (4472 to 4474) in the loop of PV-*cre*(2C) is nonviable (30). Moreover, we have demonstrated that the PV-*cre*(2C), in particular the first two As of the AAA triplet, serves as an efficient template for VPg-pUpU synthesis in vitro, which, in turn, is the primer for RNA synthesis (26, 30). Uridylylation of VPg occurs via catalysis by the RNA-dependent RNA polymerase $3D^{pol}$ in a reaction that is greatly stimulated by $3CD^{pro}$ (26).

Our previous studies have also suggested that a slide-back mechanism is involved in the nucleotidylylation of VPg, where the first UMP in VPg-pUpU is linked to VPg to form VPg-pU by using A_{4472} as the template. This is followed by a translocation of the uridylylation complex to, and base pairing with, A_{4473} and the addition of a second UMP to form VPg-pUpU (8, 30; A. V. Paul et al., unpublished data).

Available biochemical and genetic evidence has led to the suggestion that *cre* RNAs in picornaviruses are required in the sense strand for negative-strand RNA synthesis, acting in *cis* (9, 19, 30). A minigenome transcript RNA of poliovirus was used to show that the sense, but not the antisense, PV-*cre*(2C) is the functional template for the in vitro VPg uridylylation reaction (26). Given these observations, it appeared likely that poliovirus and probably all picornaviruses have acquired a mechanism to efficiently replicate their own genomic RNA via an exquisite interplay of regulatory mechanisms involving virally encoded proteins (precursors and their end products), a number of host factors, and at least three structural RNA elements.

To determine the critical structural features required for *cre* function, we have generated dual-*cre* poliovirus genomic constructs as well as a dual-*cre* (luciferase) replicon system. This strategy was based on previous observations that *cre* elements can be moved within replicons of HRV14 (18) or poliovirus (9). In our experiments, we placed second *cre*s in three different locations of the poliovirus genome. Moreover, we used *cre*s from two different picornaviruses (HRV14 and HRV2) to assess their ability to rescue the lethal phenotype caused by mutations in the native *cre* (nucleotides [nt] 4445 to 4504), mapping to the coding region of poliovirus $2C^{ATPase}$. In addition, we have analyzed the effect on in vitro VPg uridylylation of partial truncations in PV-*cre*(2C) and mutations within the core sequence in the upper stem and terminal loop of this hairpin. Our data confirm and extend recent data obtained with the HRV14 *cre* by Yang et al. (40). We also present evidence for the specific interaction between PV-*cre*(2C) and $3CD^{pro}$ (or its cleavage product $3C^{pro}$).

MATERIALS AND METHODS

Enzymes. Poliovirus RNA polymerase was expressed in *Escherichia coli* from plasmid pT5T-$3D^{pol}$, which encodes the wt sequence of $3D^{pol}$ preceded by an ATG, and was purified by the method of Pata et al. (22).

For His tag expression of $3CD^{pro}$, we used the plasmid pET21b/$3CD^{pro}$ ($3C^{pro}$/H40A). The protein was expressed in *E. coli* and purified by Ni^{2+} chromatography as described elsewhere (26). The untagged $3CD^{pro}$ (H40A) and expression vectors for His-tagged $3C^{pro}$ were gifts from C. E. Cameron (23).

Cellular PCBP2 containing a His tag was expressed in *E. coli* from plasmid pET21b/PCBP2 (this is a derivative of the plasmid pQE30-PCBP2, a gift from B. L. Semler) (21) and purified as previously described (26).

The expression of 3AB in *E. coli* and the purification of the protein were described by Lama et al. (13).

Construction of plasmids and DNA manipulation. pT7PV1(M) (36) refers to the full-length PV1(M) cDNA. Site-directed mutagenesis was performed with the QuikChange mutagenesis kit from Stratagene, and mutagenic oligonucleotides are described in Tables 1 and 2. Mutations and final constructs were verified through sequencing using the ABI Prism DNA sequencing kit.

For simplification of the nomenclature, we have numbered a functionally important sequence (consensus sequence, see below) of the *cre* element as depicted in Fig. 2. Thus, the highly conserved AAA triplet is numbered $A_5A_6A_7$. The A_5C (AAA to CAA) mutation (underlined) in PV-*cre*(2C) has been characterized previously and is referred to by Rieder et al. (30) as *mut7*. The nomenclature for dual-*cre* constructs is as follows: PV or P/L (poliovirus-luciferase) refers to the parental (full-length or replicon) plasmid, followed by the genotype

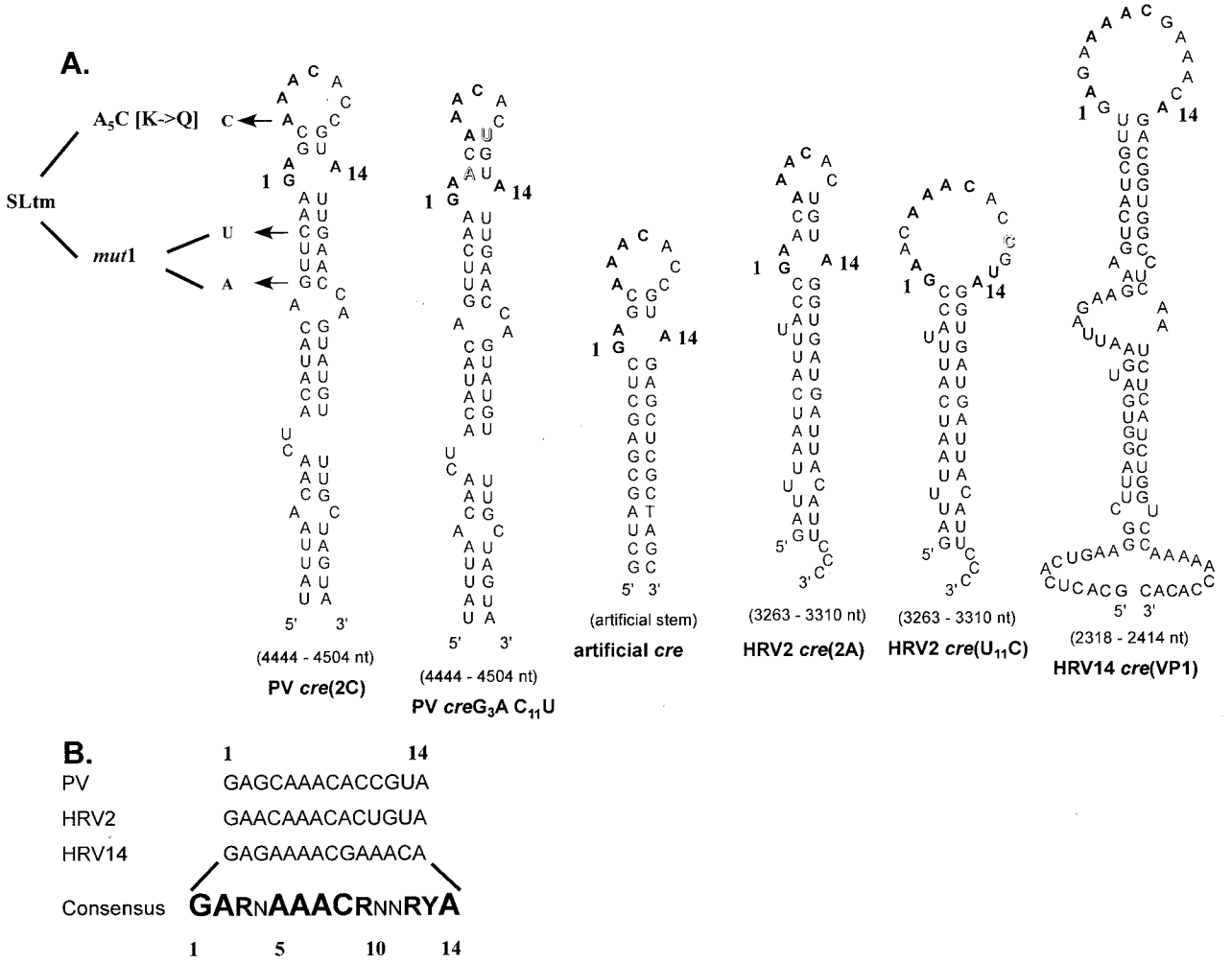

FIG. 2. Comparison of predicted *cre* structures of various picornaviruses used in this study. (A) Hairpin structures predicted by the MFOLD RNA program (Michael Zuker) for wt PV-, HRV14-, HRV2-*cre*, HRV2-*cre* carrying a $U_{11}C$ mutation which enlarges the top loop structure, and a *cre* constructed to contain 14 nt from the PV-*cre* top loop and an unrelated artificial stem. Arrows, locations of the substitutions in mutant PV-*cre*s corresponding to A_5C, $G_{4462}A$ $C_{4465}U$, and SLtm. Letters in shadow style, mutations introduced in PV-*cre* and HRV2-*cre* to alter their loop sizes. (B) Sequences of the top 14 nt of three naturally occurring picornavirus *cre*s. The consensus sequence referred to in the text as the core sequence is in boldface. The degree of conservation at each nucleotide position is indicated by the size of the letter. N, any ribonucleotide; R, purine; Y, pyrimidine.

of the native PV-*cre* (A_5C or SLtm), followed by the genotype of the "rescuer" and its insertion site in the genome (N, *Nhe*I; E, *Eco*RI; S, *Sac*I).

P/L (A_5C) is a derivative of replicon P/L (wt) (14) carrying a lethal AAA to CAA (A_5C) mutation (underlined) in the cognate PV-*cre*(2C) (see above) (30) and three unique restriction sites that are used in this study: an *Nhe*I site between the cloverleaf and IRES, a *Sac*I site at the beginning of the viral $2A^{pro}$ protein, and an *Eco*RI site next to the initiating AUG (Fig. 1). Dual-*cre* plasmids were constructed by ligation of PCR-amplified DNA fragments carrying either a point mutant PV-*cre*, an artificial *cre*, or foreign *cre* elements to the inactivated P/L (A_5C) or triple mutant $G_{4462}A$ $A_{4472}C$ $C_{4465}U$ (named SLtm for stem and loop triple mutant) replicons at either *Sac*I, *Eco*RI, or *Nhe*I restriction enzyme sites. To introduce a point mutation ($U_{11}C$) in the native HRV2-*cre*(2A), site-directed mutagenesis was performed using pT7HRV2 full-length cDNA (33) as the template and oligonucleotides described in Table 1. HRV14-*cre* was amplified with pT7HRV14 cDNA (34) as the template.

pT7PVM(S) is a full-length poliovirus cDNA clone used as a parental construct that contains an engineered restriction site (*Sac*I) between P1 and $2A^{pro}$ coding sequences (14). DNA fragments carrying the mutations in PV-, HRV2-, or HRV14-*cre* described above were generated by PCR amplification from the corresponding templates and inserted at the *Sac*I site. To assemble a dual-*cre* PV1(M) with a rescuer *cre* inserted between the cloverleaf and the IRES, a fragment between *Pml*I and *Age*I in pT7PV(M) was replaced with that of the plasmid P/L (A_5C)/PV*wt*(N).

cDNA templates corresponding to the PV-*cre*(2C) sequence (nt 4445 to 4504; Fig. 2) were obtained by PCR amplification from plasmid pT7PVM as described previously (30).

In vitro transcription, transfection, and plaque assay. All plasmids were linearized with *Dra*I. Truncated derivatives of PV-*cre* RNA used in in vitro uridylylation experiments were generated by PCR amplification using oligonucleotides described in Table 2. RNAs were synthesized with phage T7 RNA polymerase, and the RNA transcripts were transfected into HeLa R19 cell monolayers by the DEAE-dextran method as described previously (36). The incubation time was 12 h for luciferase replicons and up to 3 days for full-length viral constructs. Virus titer was determined by a plaque assay (20).

Analysis of recombinant viruses. To measure one-step growth kinetics, we used HeLa R19 monolayers (5×10^6 cells) infected with virus at a multiplicity of infection of 5 to 10. The plates were incubated at 37°C, and the infected cells were harvested at 0, 1, 2.5, 3, 5, 8, and 12 h postinfection. The virus yield of the cell lysates was determined by plaque assay.

TABLE 1. Oligonucleotides used for mutagenesis and cloning (involving PCR amplification)

Oligonucleotide	Sequence (5′–3′)
PV*cre* (SacI) forward	GCC GAG CTC ACA ACC TAT GGG TTC GGA ACT ATT AAC AAC TAC ATA C
PV*cre* (SacI) reverse	GC GAG CTC TAC TAG CAA ACA TAC TGG
HRV14*cre* (SacI) forward	GCC GAG CTC ACA ACC TAT GGG TTC GGA GCA CTC ACT GAA GGC TTA G
HRV14*cre* (SacI) reverse	GGC GAG CTC TTT TTG TGT GTG TTT TGG
HRV2*cre* (SacI) forward	GCC GAG CTC ACA ACC TAT GGG TTC GGA GAT TTA ATC ATT TAC CGA AC
HRV2*cre* (SacI) reverse	GGC GAG CTC GGG AAT GTA ATC ATC ACC
HRV2*cre* $U_{11}C$ forw. (QM)[a]	ATT TAC CGA ACA AAC ACC GTA GGT GAT GAT TAC
PV*cre* (EcoRI) forward	CGG AAT TCA CTA TTA ACA ACT ACA TAC AG
PV*cre* (EcoRI) reverse	CGG AAT TCC CCA AAG CCG TAA GTC GTT ACT AGC AAA CAT ACT GG
PV*cre* G_3A $C_{11}U$ forw. (QM)	CAT ACA GTT CAA GAA CAA ACA CTG TAT TGA ACC AGT ATG
PV*cre* $A_{14}C$ forward (QM)	CAA GAG CAA ACA CCG TCT TGA ACC AGT ATG TTT G
PV*cre* G_1A forward (QM)	CTA CAT ACA GTT CAA AAG CAA ACA CCG TAT TG
PV*cre* G_1C forward (QM)	CTA CAT ACA GTT CAA CAG CAA ACA CCG TAT TG
PV*cre* G_1U forward (QM)	CTA CAT ACA GTT CAA TAG CAA ACA CCG TAT TG
PV*cre* $A_{14}G$ forward (QM)	CAA GAG CAA ACA CCG TGT TGA ACC AGT ATG TTT G
PV*cre* $A_{14}U$ forward (QM)	CAA GAG CAA ACA CCG TTT TGA ACC AGT ATG TTT G
PV/Luc+(NheI) forw. (QM)	GTT TTA TAC TCC CTT CCC GCT AGC TTA GAC GCA CAA AAC CAA G
PV*cre* (NheI) forward	CTA GCT AGC ACT ATT AAC AAC TAC
PV*cre* (NheI) reverse	CTA GCT AGC TAC TAG CAA ACA TAC
Artificial *cre* (NheI) forward	CTA GCT AGC GAG CTC GAG CAA ACA CCG TAG AGC
Artificial *cre* (NheI) reverse	GAT GCT AGC GAG CTC TAC GGT GTT TGC TCG AGC
Artificial *cre* A_5C(NheI) forw.	CTA GCT AGC GAG CTC GAG CCA ACA CCG TAG AGC
Artificial *cre* A_5C(NheI) rev.	GAT GCT AGC GAG CTC TAC GGT GTT GGC TCG AGC
PV*cre* (SLtm) forward (QM)	CTA TTA ACA ACT ACA TAC AAT TTA AGA GCC AAC ACC GTA TCG AAC

[a] QM, oligonucleotide used for QuikChange mutagenesis.

VPg uridylylation assay. The reaction mixture contained 50 mM HEPES, pH 7.5, 3.5 mM magnesium acetate, 1 μg of purified $3D^{pol}$, 2 μg of synthetic poliovirus VPg, ~0.75 μCi of [^{32}P]UTP (3,000 Ci/mmol; DuPont NEN), 10 μM unlabeled UTP, and 0.5 μg of template RNA transcribed in vitro from a PCR product containing *cre* stem-loop RNA or various PV1(M) constructs (26). Unless otherwise indicated either 1 μg of $3CD^{pro}$ or 0.5 μg of $3C^{pro}$ was added to the reaction mixture. After incubation at 34°C for 30 min, the reaction was stopped by the addition of 5 μl of gel loading buffer. The samples were then analyzed on Tris-Tricine sodium dodecyl sulfate-polyacrylamide gel electrophoresis gel (Bio-Rad) with 13.5% polyacrylamide. Gels were dried without fixing and autoradiographed. The incorporation of [^{32}P]UMP into VPg-pU and VPg-pUpU was measured on a phosphorimager (Molecular Dynamics; Storm 860).

Luciferase assay. After being transfected with replicon RNA, the monolayer cultures (35-mm-diameter dishes) of HeLa R19 cells were incubated at 37°C in standard tissue culture medium. After 12 h, the growth medium was removed from the dishes, and the cells were washed gently with 2 ml of phosphate-buffered saline. HeLa cell dishes were overlaid with 300 μl of "passive" lysis buffer supplied by Promega (catalog no. E194A) and rocked at room temperature for 15 min, after which the lysate was transferred to a tube. Fifty microliters of luciferase assay reagent (Promega; luciferase assay system catalog no. E1501) was mixed with 20 μl of lysate, and the firefly luciferase activity was measured in an Optocomp I luminometer (MGM Instruments, Inc.).

Electrophoretic mobility shift and filter binding assays. Assays were performed as described previously with some modifications (10, 39). The radiolabeled RNA *cre* probes were generated by in vitro transcription in the presence of [^{32}P]UTP by using templates generated through PCR with primers encoding the T7 polymerase promoter. To prevent nonspecific binding of the proteins to the RNA, an excess of nonspecific RNA (10 μg of tRNA) was added to all reaction mixtures. Radiolabeled PV-*cre*(2C) RNA (7 nM; nt 4445 to 4504; Fig. 2) was added to the binding buffer (5 mM MOPS [pH 7.4], 25 mM KCl, 2 mM $MgCl_2$, 20 mM dithiothreitol) containing either HeLa S10 extract or various amounts of recombinant protein, i.e., His-tagged $3C^{pro}$, $3CD^{pro}$ with or without the His tag, $3D^{pol}$, 3AB, or PCBP2), and incubated for 10 min at 30°C. Reactions were stopped by the addition of glycerol to a final concentration of 10%, and reaction products were loaded on a native 0.5× Tris-borate-EDTA–5% polyacrylamide (40:1) gel containing 5% glycerol. The cellular extracts (cytoplasmic S10 extract) were prepared as described previously (20). In filter binding assays, the reactions were performed in duplicate. A 20-μl reaction mixture containing various amounts of proteins plus 1 μl of radiolabeled RNA (7 nM) was incubated for 15 min at room temperature, after which aliquots were filtered at low negative pressure through prewetted nitrocellulose membranes (pore size, 0.45 μm; Schleicher & Schuell). Beneath the nitrocellulose membrane a nylon membrane (Boehringer Mannheim) and then a 3MM cellulose membrane were placed (23). Filters were washed once with wash buffer (20 mM HEPES-KOH [pH 6.8], 1 mM magnesium acetate, 10 mM 2-mercaptoethanol) and dried, and the radioactivity was measured by liquid scintillation counting in the presence of EcoLite scintillation cocktail (ICN).

RNA structure prediction. We used the MFOLD program designed by Michael Zuker (http:/www.bioinfo.rpi.edu/applications/mfold).

RESULTS

Rescue of a replication-incompetent P/L (A_5C) replicon with a second copy of *cre* of different picornavirus origin. Previously, we demonstrated that the conserved $A_5A_6A_7$ sequence of the PV-*cre*(2C) plays a role in the replication of poliovirus

TABLE 2. Oligonucleotides used for the synthesis of truncated PV-*cre*(2C)

Oligonucleotide	Sequence (5′–3′)
T7 Δ1*cre* forward	GGT GCC GGC TAA TAC GAC TCA CTA TAG GCT ACA TAC AGT TCA AGA GCA AAC
Δ1*cre* reverse	AAG AAT TCC AAA CAT ACT GGT TCA ATA CGG TGT TTG CTC TTG AAC TGT
T7 Δ2*cre* forward	GGT GCC GGC TAA TAC GAC TCA CTA TAG GTT CAA GAG CAA AC
Δ1*cre* reverse	CAA GAA TTC CTA GGG TTC AAT ACG GTG TTT GCT CTT GAA CCT ATA G
T7 Δ3*cre* forward	GTG CCG GCT AAT ACG ACT CAC TAT AGG CAA ACA CCG TAT TG
Δ3*cre* reverse	AAG AAT TCC TAG GGT TCA ATA CGG TGT TTG CCT ATA GT

RNA (30). For example, the A_5C mutation in the loop of PV-*cre*(2C) rendered the resulting virus nonviable, and no revertants could be recovered even after five blind passages in HeLa R19 cells. In agreement with these findings a P/L (A_5C) replicon carrying the same mutation in the endogenous PV-*cre*(2C) showed little luciferase activity after transfection (see below). The A_5C mutation leads to amino acid change $K_{117}Q$ in $2C^{ATPase}$. Available evidence suggests that this change does not significantly interfere with the $2C^{ATPase}$ activity (29, 30) and that the effect of the mutation is due to the inactivation of the *cre* signal. To provide experimental evidence for this assumption and to allow for extensive genetic analysis of the *cre* element, we introduced a second copy of wt PV-*cre* (63 nt from 4444 to 4506) at different locations (Fig. 1). For example, the wt *cre* was inserted between the coding sequence for the C terminus of P1/luciferase and that for the N terminus of $2A^{pro}$ (Fig. 1, *Sac*I site inserts). To facilitate the processing of the modified polyprotein, a $2A^{pro}$ cleavage site was introduced between the translation product of the new *cre* and the P1/luciferase so that after translation the extra 21 amino acids encoded by the *cre* would be cleaved out of the polyprotein. As shown in Fig. 3A, the second copy of wt PV-*cre* at this position can restore the replication of an inactive P/L (A_5C) replicon to that of the wt P/L (Fig. 3A, compare lanes 3 and 5 with lane 1). Furthermore, a dual-*cre* replicon carrying two mutant copies of A_5C *cre* (Fig. 3A, lanes 21 and 22) failed to show any luciferase activity above the background signal. The background signal was determined by repeating the experiments in the presence of 2 mM guanidine-HCl, an inhibitor of poliovirus RNA synthesis (Fig. 3A, even-numbered lanes). Taken together, the data, in agreement with previous results, suggest that (i) the 63-nt PV-*cre* is a functional signal for the replication of poliovirus RNA in vivo (9, 26, 30), (ii) the function of PV-*cre* is independent of the cognate amino acid sequence of the viral $2C^{ATPase}$ protein, and (iii) a functional *cre* element can be moved to a different location within the poliovirus genome (9).

We have recently shown that *cre* elements from HRV14 and poliovirus can be functionally exchanged in our in vitro uridylylation assays using poliovirus $3D^{pol}$ (26). Therefore, we were interested in determining whether heterologous *cre* elements could rescue the replication of a P/L (A_5C) replicon carrying a lethal mutation in the native PV-*cre*(2C) by engineering the foreign *cre* elements into dual-*cre* RNAs. As shown in Fig. 3A (lane 13) HRV14-*cre* restored the replication level of this replicon to 70% of that of wt dual-*cre* (lane 5). HRV2-*cre*, on the other hand, barely (3%) rescued the replication of the dual-*cre* replicon (Fig. 3A, compare lanes 5 and 9). This is in agreement with our findings that HRV2-*cre*(2A) is a very poor template for poliovirus $3D^{pol}$ in VPg uridylylation (A. V. Paul and E. Wimmer, unpublished data).

Rescue by genetically altered PV-*cre*(2C), HRV2-*cre*(2A), or artificial *cre*'s. As shown in Fig. 2A, PV-, HRV2-, and HRV14-*cre* differ significantly from each other in their primary nucleotide sequences. However, we have highlighted a consensus sequence of 14 nt (named core in this paper; Fig. 2B) that is highly conserved among all *cre* structures. Curiously, although HRV2-*cre* appears to be more similar to PV-*cre* than to HRV14-*cre* in its core sequence, HRV14-*cre* was much more efficient in rescuing a debilitated (A_5C) dual-*cre* replicon than HRV2-*cre* (Fig. 3A, compare lane 5 with lanes 9 and 13). A

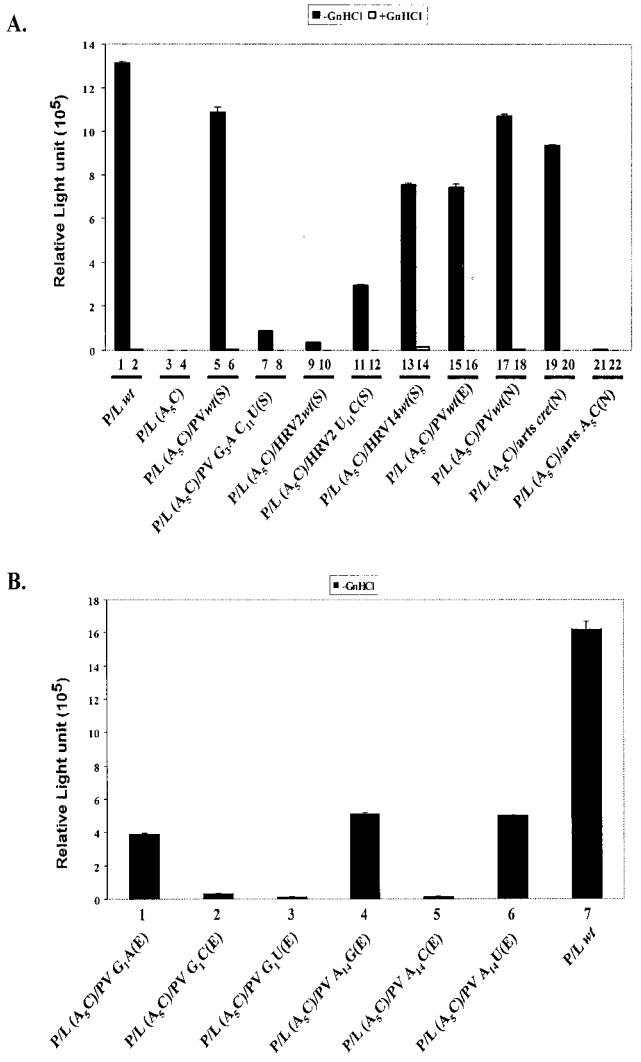

FIG. 3. Luciferase activities of various P/L replicons as a measure of RNA replication. (A) RNAs from dual-*cre* P/L replicons with second rescuer *cre* elements derived from poliovirus, HRV2, or HRV14. Transfection of RNA and luciferase activity measurements are described in Materials and Methods. Even-numbered lanes, transfections repeated in the presence of 2 mM guanidine-HCl (GnHCl). arts, artificial. (B) Dual-*cre* luciferase replicons with the rescuer *cre* from poliovirus carrying point mutations in G_1, A_2, and A_{14} in the core *cre* sequence were tested for their ability to replicate in HeLa R19 cells. The nomenclature is as follows. P/L refers to the parental replicon plasmid followed by A_5C when it carries an inactivating mutation in the $2C^{ATPase}$ coding sequence. This is followed by the sequences of the rescuer *cre* and the insertion site (N, *Nhe*I; E, *Eco*RI; S, *Sac*I).

major difference between the upper portions of HRV2-*cre* and HRV14-*cre* is the size of the loop. We were interested to test the hypothesis that a predicted "tight" structure in the core sequence of HRV2-*cre* that leads to base pairing of A_5 prevented it from being an efficient rescuer in the context of the poliovirus genome. Therefore, a point mutation ($U_{11}C$) was engineered into the core sequence of wt HRV2-*cre* so that the predicted secondary structure for the altered HRV2-*cre* resembles that of the HRV14-*cre* top loop. Indeed, the altered HRV2-*cre* was about 10-fold more efficient in rescuing a de-

bilitated (A_5C) PV-*cre* than the wt HRV2-*cre* (Fig. 3A, compare lane 5 with lanes 9 and 11). The reason why the recovery of luciferase activity is still low compared to that for PV-*cre* or HRV14-*cre* is not known but is undoubtedly related to the *cre* structure and its interaction with the proteins involved in uridylylation. Perhaps the presence of an unpaired U residue in the upper region of the stem is responsible for the low activity in the context of a poliovirus genome (30). In some cases, a relationship between higher-order structure and function can be predicted. For example, a mutant PV-*cre* carrying two point mutations (G_3A and $C_{11}U$) in its core sequence has a predicted loop structure identical to that of wt HRV2-*cre*. Indeed, this variant PV-*cre* produced only 8% luciferase activity when used as a rescuer *cre* in the dual-*cre* replicon (Fig. 3A; compare lanes 5 and 7).

The core sequences of PV-, HRV2-, and HRV14-*cre* are relatively more conserved than the rest of the hairpin sequence (Fig. 2B). Along with the $A_5A_6A_7$ sequence, the first two (G_1 and A_2) nucleotides and the last (A_{14}) nucleotide were among the most conserved. Mutations A_2C and A_2U did not influence the ability of the second *cre* element to rescue a lethal mutation in the cognate *cre* (data not shown). On the other hand, some G_1 and A_{14} mutants [P/L (A_5C)/PV G_1A(E), P/L (A_5C)/PV $A_{14}G$(E), and P/L (A_5C)/PV $A_{14}U$(E)] displayed significant reduction in the level of replication compared to wt P/L (Fig. 3B, compare lane 7 with lanes 1, 4, and 6). Interestingly, other G_1 mutants [P/L (A_5C)/PV G_1C(E), P/L (A_5C)/PV G_1U(E), and A_{14}(P/L) A_5C/PV $A_{14}C$(E)] exhibited very little if any replication signal (Fig. 3B, compare lane 7 with lanes 2, 3, and 5). Currently, we have no explanation for the remarkable intolerance for transversions at the G_1 position, but it is likely related to the reduced ability of this mutant to bind $3CD^{pro}$ (see Fig. 9C). A possible explanation for the relatively high activity of the $A_{14}U$ replicon (lane 6), compared to that of the $A_{14}C$ replicon (lane 5) will be given in Discussion.

The stem structures beneath the core sequence display the biggest diversity among the *cre* structures studied. To evaluate the role of sequences located in the stem region beneath the core sequence, we constructed an artificial *cre* consisting of an authentic PV-*cre* core (G_{4468}AGCAAACACCGUA$_{4481}$) sequence and an artificial stem of unrelated nucleotide sequence (Fig. 2A). This stem was designed to accommodate an *Nhe*I restriction site for easy insertion between the cloverleaf structure and the IRES element in the 5′ NTR (Fig. 1) and will be discussed below. As seen in Fig. 3A, this artificial *cre*, when inserted into the P/L (A_5C) replicon genome, efficiently rescued the lethal phenotype caused by an A_5C mutation in the native PV-*cre*. This observation suggests that the structure (i.e., scaffolding) of the stem beneath the core sequence of various *cre*s is more important than its nucleotide sequence.

Rescue of replication by wt PV-*cre*(2C) placed at different locations in the P/L replicon. To determine if the genomic position of PV-*cre* affects its role in poliovirus replication, we tested the effect of a rescuing a *cre* element at three locations in the dual-*cre* replicon genome: inside the polyprotein open reading frame [ORF; P/L (A_5C)/PV*wt*(S)], in the beginning of the ORF [P/L (A_5C)/PV*wt*(E)], and in the noncoding region in the 5′ NTR between the cloverleaf and the IRES element [P/L (A_5C)/PV*wt*(N)]. The result showed that the location of the *cre* elements has very little effect on the replication of the genome (Fig. 3A, compare lane 1 with lanes 5, 15, and 17).

The efficient rescuing function of the poliovirus *cre* element outside the ORF was surprising. As mentioned above, even an artificial *cre* element inserted into the *Nhe*I site allowed replication of the RNA carrying a lethal A_5C mutation in the cognate *cre* element (Fig. 3A, compare lanes 17 and 19). In contrast, an artificial *cre* with an A_5C mutation in the core sequence did not rescue replication (Fig. 3A, compare lanes 17 and 21), an observation proving that RNA synthesis strictly depended on a functional *cre*, regardless of its locus in the genome.

In vitro uridylylation of VPg using dual-*cre* poliovirus RNAs as templates. We have previously developed an in vitro assay in which the viral RNA-dependent RNA polymerase $3D^{pol}$ transfers a UMP to the tyrosine residue in the small viral protein VPg, by using poly(A) as the template (27). We further made the discovery that such a reaction was stimulated (by 1 order of magnitude) by the presence of viral protein $3CD^{pro}$ when genome RNA or the *cre* sequence was used as the template (26, 30). Enhancement of uridylylation was observed also with $3C^{pro}$ (23). Since the stimulatory activity of $3C^{pro}$ is more reproducible than that of the much larger (His-tagged) $3CD^{pro}$, we used $3C^{pro}$ in uridylylation reactions catalyzed by dual-*cre* replicon RNAs. As shown in Fig. 4A, in the absence of $3C^{pro}$, there was little uridylylation of VPg by $3D^{pol}$ when any of the different RNAs were used as the template (Fig. 4A, lanes 2, 4, 6, 8, 10, and 12). The P/L (A_5C) replicon RNA carrying the lethal A_5C mutation in *cre*(2C) failed to function as a template for the uridylylation of VPg (Fig. 4A, lane 1), as expected (30). In the presence of $3C^{pro}$, only RNAs with a functional *cre* were able to direct significant uridylylation of VPg above the background level (Fig. 4A, lanes 3, 5, 7, 9, 11, and 13). This is in good agreement with the observed replication levels of these replicons in tissue culture, as determined by measuring luciferase activity (Fig. 3A, lanes 1, 5, 9, 11, and 13). This was also observed for the mutated HRV2-*cre* ($U_{11}C$), which is a better template for uridylylation of VPg in vitro than the dual-*cre* replicon carrying wt HRV2-*cre*(2A) (Fig. 4A, compare lanes 9 and 13). Reciprocally, when the loop (14 nt) of PV-*cre*(2C) was converted to that of HRV2-*cre*(2A), the hybrid *cre* (PV G_3A $U_{11}C$) not only displayed a much-reduced ability to replicate (Fig. 3A, lane 7) but also was a poor template for the uridylylation of VPg in vitro (Fig. 4B, lane 4).

The different location of the rescuer copy of PV-*cre*(2C) did not influence significantly its template activity for the uridylylation of VPg in vitro, as shown in Fig. 4B. The dual-*cre* replicons that displayed wt P/L luciferase activity (Fig. 3A, lanes 1, 5, 15, and 17) in HeLa cells also exhibited VPg uridylylation levels similar to that of the wt construct (Fig. 4B, lanes 1, 3, 5, and 6). This further suggests that the *cre*(2C) RNA sequence functions as a replication signal independently of the function of the viral $2C^{ATPase}$ and local RNA-RNA interactions. Not surprisingly, the dual-*cre* replicon carrying the artificial *cre* as the rescuer is a good template for both the uridylylation of VPg in vitro (Fig. 4B, lane 7) and replication in HeLa R19 cells (Fig. 3A, lane 19).

One-step growth curve of dual-*cre* polioviruses. To examine to what extent rescue by cognate or foreign *cre*s influences virus yield, we tested virus production with genomes carrying a

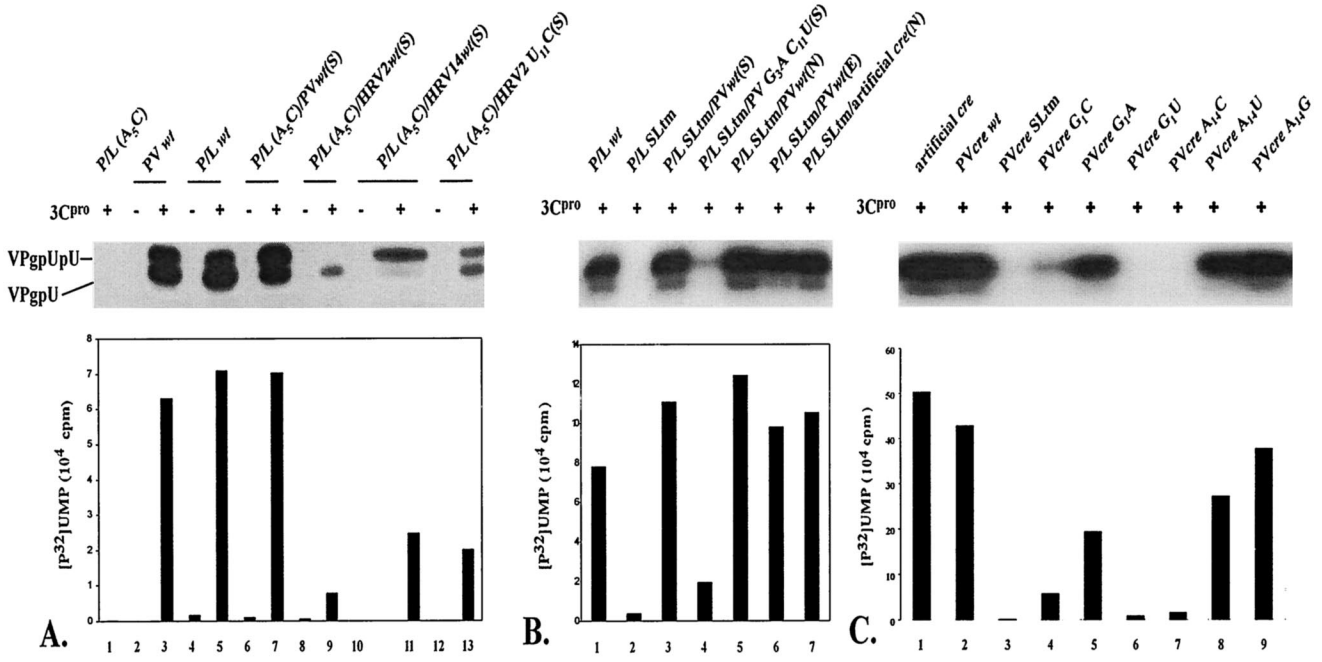

FIG. 4. In vitro uridylylation of VPg using either a dual-*cre* P/L replicon or mutated PV-*cre* RNAs as the template. Uridylylation reactions were performed as described in Materials and Methods. (A) Dual-*cre* replicons carrying a lethal (A_5C) mutation in the $2C^{ATPase}$ coding sequence with a rescuer *cre* from HRV14 or HRV2 or a mutant $U_{11}C$ HRV2-*cre* (predicted by the Zuker program to enlarge the terminal loop of HRV2-*cre* to resemble that of HRV14-*cre*). (B) VPg uridylylation using inactivated dual-*cre* (SLtm; triple mutant) replicons as templates and the rescuer wt PV-*cre* inserted at different locations. (C) Mutant or wt *cre* RNAs as templates in VPg uridylylation.

lethal A_5C mutation in PV-*cre*(2C) as well as a second *cre* (PV-*cre*, HRV2-*cre*, HRV14-*cre*, or HRV2-*cre* $U_{11}C$) element. Two locations of the second *cre* were used for these experiments: (i) between the P1 and P2 coding sequences and (ii) between the cloverleaf and the IRES element in the 5′ NTR. As shown in Fig. 5, the dual-*cre* viruses with a second copy of functional viral *cre* displayed similar growth kinetics. These results suggest that, in vivo, the uridylylation of VPg might not be the rate-limiting step of poliovirus RNA replication. Note that HRV2-*cre*, a weaker template for in vitro VPg uridylylation by poliovirus $3D^{pol}$ (Fig. 4A, lane 9), still stimulated the dual-*cre* virus to amplify by over 2 orders of magnitude at 12 h postinfection (Fig. 5). The results also suggested that the location of the rescuer *cre* has little effect on the recovery of virus, as PV (A_5C)/PV*wt*(N) has growth kinetics similar to those of PV (A_5C)/PV*wt*(S) and both proliferated at a rate comparable to that for wt PV (Fig. 5).

To exclude the possibility that the insertion of a second *cre* impairs replication of the resulting virus, we also inserted the above *cre* elements into the wt poliovirus genome and studied the resulting viruses in one-step growth experiments. As shown in Fig. 5, a dual-*cre* virus carrying wt *cre* in the 2C coding region grew just as well as wt poliovirus, regardless of the content of the second *cre*, and slightly better than the dual-*cre* viruses carrying the A_5C mutation.

The growth phenotypes of the constructs carrying mutations in the *cre* element could also be due to rapid mutation to wt sequences or second-site suppressor mutations. Sequence analysis of the genomic RNAs recovered after two passages in HeLa cells did not reveal changes in the *cre* sequences. This result excludes direct reversion, but it does not eliminate second-site suppressor mutations. This interesting possibility is currently under investigation.

In vitro uridylylation of VPg using PV-*cre* G_1 and A_{14} mutants and artificial *cre* RNAs as templates. We were also interested in the ability of PV-*cre*'s to direct VPg uridylylation when either the G_1 or A_{14} nucleotides were altered. As shown in Fig. 4C, transversions at these positions caused a strong defect in the protein priming reaction. Mutant PV-*cre*s carrying either G_1C or G_1U or $A_{14}C$ mutations in the core *cre* sequence lost more than 90% of VPg uridylylation activity compared to the *wt* PV-*cre* (Fig. 4C, compare lane 2 with lanes 4, 6, and 7), whereas PV-*cre* $A_{14}U$ is about 50% as functional as wt PV-*cre* (Fig. 4C, compare lanes 8 and 2). On the other hand, transitions are better tolerated at both nucleotide positions: PV-*cre* G_1A and PV-*cre* $A_{14}G$ retained 50 and 90% of wt PV-*cre* activity for the uridylylation of VPg in vitro, respectively (Fig. 4C, compare lane 2 with lanes 5 and 9). As a negative control, mutant PV (SLtm) (Fig. 2) was constructed to carry the debilitating A_5C change and two point mutations in the upper stem region ($G_{4462}A$ and $C_{4465}U$); these three mutations are predicted to alter the secondary structure of *cre* drastically. As expected, PV (SLtm) showed only a background level signal for the in vitro uridylylation of VPg (Fig. 4C, lane 3), which is in accordance with previous findings with full-length viral RNA and poliovirus replicons (9, 30). These results suggest a preference for purine at the N_1 and N_{14} nucleotide positions in the core sequence of PV-*cre*(2C), specifically a G_1 and an A_{14}.

We also tested our artificial *cre*, carrying the wt core se-

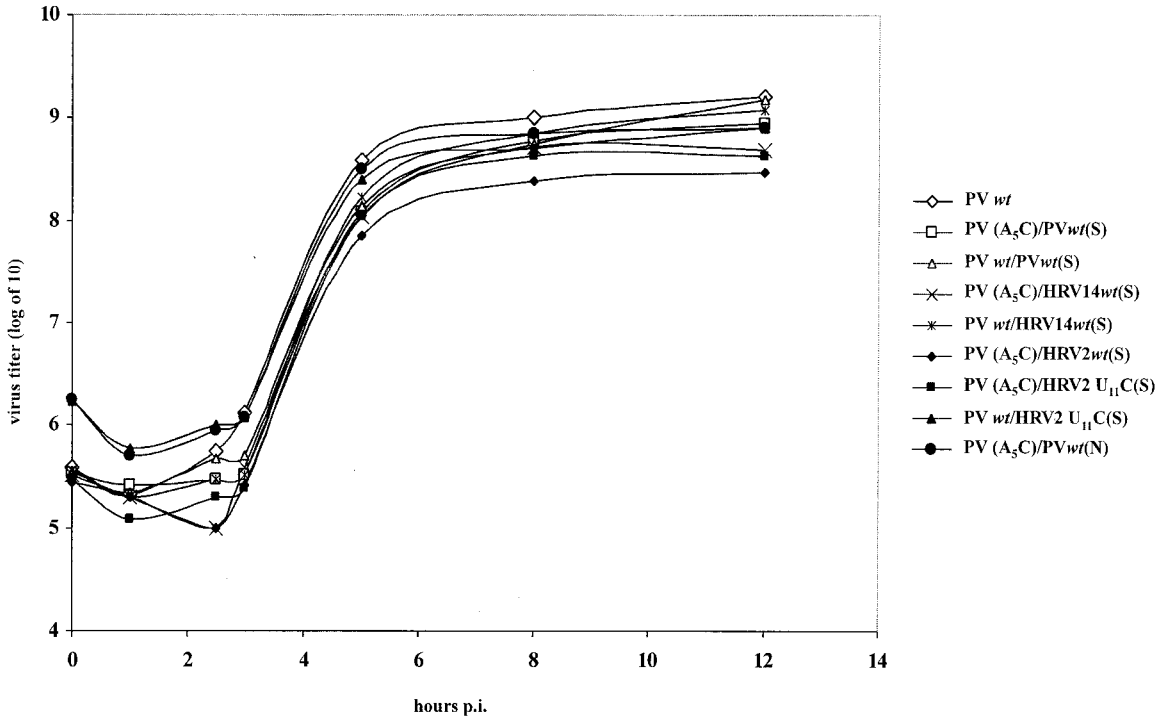

FIG. 5. One-step growth curves for various dual-*cre* polioviruses. HeLa R19 cells were infected with virus derived from wt and mutant poliovirus cDNA plasmids, and the virus yield was determined at the indicated time points (see Materials and Methods).

quence from PV-*cre*(2C) and a stem of unrelated nucleotide sequence, in the in vitro VPg uridylylation assay. As shown in Fig. 4C (compare lanes 1 and 2), the artificial *cre* is as functional as the wt PV-*cre* for directing the synthesis of VPg-pU and VPg-pUpU under the experimental conditions, in agreement with our data for the dual-*cre* replicon shown in Fig. 3A (lane 19).

Analysis of full-length poliovirus genomes carrying mutations within the loop of PV-*cre*(2C). Further characterization of the effect of mutations within the core PV-*cre* sequence was carried out by using mutant full-length polioviruses. The growth phenotype and uridylylation activities of these full-length constructs are shown in Fig. 6A and B, respectively. Similar to the wt, C_8A, A_9G, and C_8U A_9G mutants developed complete cytopathic effect (CPE) after 24 h of incubation at 37°C posttransfection. A delay in the appearance of CPE was observed with the A_9U mutant, an observation suggesting that this mutant RNA may be impaired in replication. We suspected that the inefficient replication may lead to a reversion or other genetic alterations. This was confirmed by sequence analysis (reverse transcription-PCR) of RNA extracted from the virus that was collected after three passages following the original transfection. It reveals a reversion at the site of mutagenesis (U_9A) to the original codon (resulting in a change from Leu_{118} to His). In addition, we detected a change at position A_7G in the core sequence (synonymous mutation). No CPE was detected with $C_{10}U$ $C_{11}U$ mutant RNA even after three additional blind passages in HeLa R19 cells. This result is not unexpected since the substitutions introduced into this double mutant are likely to lead to base pairing with the critical A_5 and A_6 nucleotides in the core *cre* sequence. This is supported only by computer-aided folding; no biochemical evidence has been generated. The $C_{10}U$ $C_{11}U$ mutation also greatly reduces the yield of VPg-pU and VPg-pUpU products in in vitro uridylylation (Fig. 6B). The results are also consistent with the data from dual-*cre* replicons [P/L (A_5C)/PV G_3A $C_{11}U$(S)] shown in Fig. 3A, where a mutation in the PV-*cre* loop which reduces the size of the terminal loop reduced luciferase activity 10-fold relative to that for the P/L carrying wt PV-*cre*. However, since the double mutation changes the amino acid sequence from $H_{118}R_{119}$ to $H_{118}C_{119}$, we cannot rule out the possibility that this may critically impair $2C^{ATPase}$ function. The $C_{10}U$ and $C_{11}U$ mutations have not yet been tested in a dual-*cre* construct.

All mutant versions of the full-length RNAs tested above are functional templates in the in vitro VPg uridylylation reaction (Fig. 6B). However, smaller amounts of VPg-pU and VPg-pUpU products were produced than were produced with wt PV1 RNA (Fig. 6B, compare lane 1 with lanes 3, 5, 7, 9, and 11). Among them, only one ($C_{10}U$ $C_{11}U$ mutant; 10% of wt activity in uridylylation; Fig. 6B, compare lane 1 with lane 7) rendered the genome nonviable. Polypeptide $3CD^{pro}$ significantly stimulated uridylylation in all cases, as its absence greatly reduced synthesis of the VPg-pU and VPg-pUpU products (Fig. 6B, lanes 2, 4, 6, 8, 10, and 12). The existence of viable mutants containing amino acid changes at His_{118} in $2C^{ATPase}$ suggests that this His residue is not essential for $2C^{ATPase}$ function in the replication of poliovirus (Fig. 6A). However, whereas the His_{118}Arg change was tolerated, a the His_{118}Leu change produced a replication phenotype that led to

A

	Core PV*cre*(2C) sequence (S K_{117} H_{118} R)	Amino acid change in $2C^{ATPase}$	pfu/ml	Revertants (RT-PCR at 3rd passage)
WT	G AGC AAA CAC CGU A	None	9.8×10^7	No
(C_8A)	G AGC AAA ***A***AC CGU A	H → N	7.0×10^7	No
(A_9G)	G AGC AAA C***G***C CGU A	H → R	5.4×10^7	No
($C_{10}U$, $C_{11}U$)	G AGC AAA CA***U U***GU A	R → C	-	No
(A_9U)	G AGC AAA C***U***C CGU A	H → L	6.2×10^4	Yes ($\frac{K_{117}H_{118}}{}$ G AGC AA***g*** C ***a***C CGU A)
(C_8U, A_9G)	G AGC AAA ***UG***C CGU A	H → C	4.8×10^7	No

B

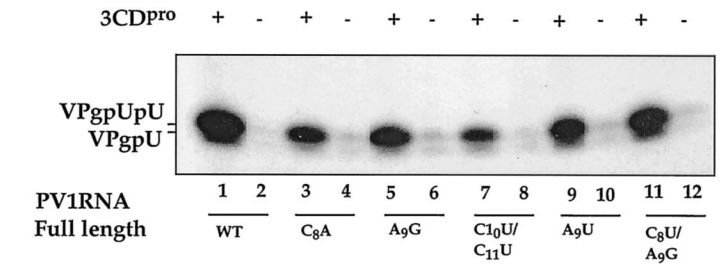

FIG. 6. Summary of the effect of nucleotide substitutions within the PV-*cre*(2C) loop in full-length PV1(M) genome RNA on genome replication and uridylylation. (A) Phenotypic properties of viruses derived from transfection experiments with HeLa R19 cells. Following transfection into HeLa cells the cell lysates were subjected to three additional passages and the viral RNAs were sequenced following reverse transcription-PCR, as described in Materials and Methods. The letters above the nucleotides indicate the deduced amino acid sequence and its location within $2C^{ATPase}$. Mutations or reversions in nucleotides are in boldface and italics. Nucleotide reversions are shown with lowercase letters. (B) VPg uridylylation was assayed as described in Materials and Methods with full-length wt or mutant RNAs as templates. Where indicated, poliovirus $3CD^{pro}$ was added to the reaction mixtures.

reversion to the original codon and amino acid. Since this reversion is accompanied by a synonymous change in the preceding codon, it is impossible to decide whether the growth phenotype of the A_9U mutant resulted from the amino acid change, from the structure of the *cre*, or both. Finally, a G_1U mutation in cognate PV-*cre*(2C) of poliovirus RNA rendered the genome nonviable, even after three blind passages in HeLa cells (data not shown). Taken together, the data support the hypothesis that critical features of the *cre* required for replication are contained in a 14-nt core sequence in the apical portion of the RNA stem-loop.

Minimal length of PV-*cre*(2C) required for uridylylation. We have performed experiments to analyze the relationship between the length of the stem in PV-*cre*(2C) and VPg uridylylation. Two truncated PV-*cre* RNAs were synthesized in vitro and tested as templates in the in vitro uridylylation assays. As shown in Fig. 7, both RNAs were able to serve as templates, but the yield was reduced to 70 to 80% of that with the wt PV-*cre* [Δ1 PV-*cre*(2C)] and to 25% of that with Δ2 PV-*cre*(2C) (compare lane 1 with lanes 2 and 3). The data indicate that the upper stem and loop of PV-*cre*(2C) carry the minimal structural determinants for the assembly of a uridylylation-competent complex. On the other hand, an RNA spanning the sequence 4470 to 4504 [Δ3 PV-*cre*(2C)] of the poliovirus genome is totally inactive as a template in the reaction (Fig. 7, compare lanes 1 and 4), suggesting that the sequence determinants contained in this region must be contained within a certain spatial arrangement to be recognized by the proteins of the uridylylation complex.

Proteins binding to the poliovirus *ori*I [PV-*cre*(2C)]. The function of PV-*cre*(2C) is likely to involve an RNP complex consisting of more than one protein. As shown previously, PV-*cre*(2C) serves as an efficient template for $3D^{pol}$-catalyzed VPg uridylylation only if $3CD^{pro}$ or $3C^{pro}$ is present (23, 26) (see our results above). We therefore used a binding assay to test interactions between viral and possibly cellular polypeptides and PV-*cre*(2C).

We first investigated if nonstructural proteins that originated from the P3 region of the polyprotein ($3CD^{pro}$, 3AB, and $3D^{pol}$) and the cellular protein PCBP2 possess specific affinity to PV-*cre*(2C) by gel shift assays, carried out in the presence of a 1,000-fold excess of nonspecific competitor tRNA (10). Purified polypeptide 3AB, known to be a nonspecific RNA-binding protein (25, 38), does not bind to PV-*cre*(2C) under these conditions (Fig. 8A, compare lane 1 with lane 6). In contrast, $3CD^{pro}$ and its cleavage product $3C^{pro}$ retarded the mobility of the labeled probe in the presence of the 1,000-fold excess of tRNA (Fig. 8A, lanes 2 and 4, respectively). Gel shift assays carried out with increasing amounts of $3CD^{pro}$-His showed that the amount of RNP complex formed is dependent on the concentration of the protein in the reaction mixture up to about 400 nM $3CD^{pro}$ (Fig. 8B, lanes 2 to 7, and 9A). This is

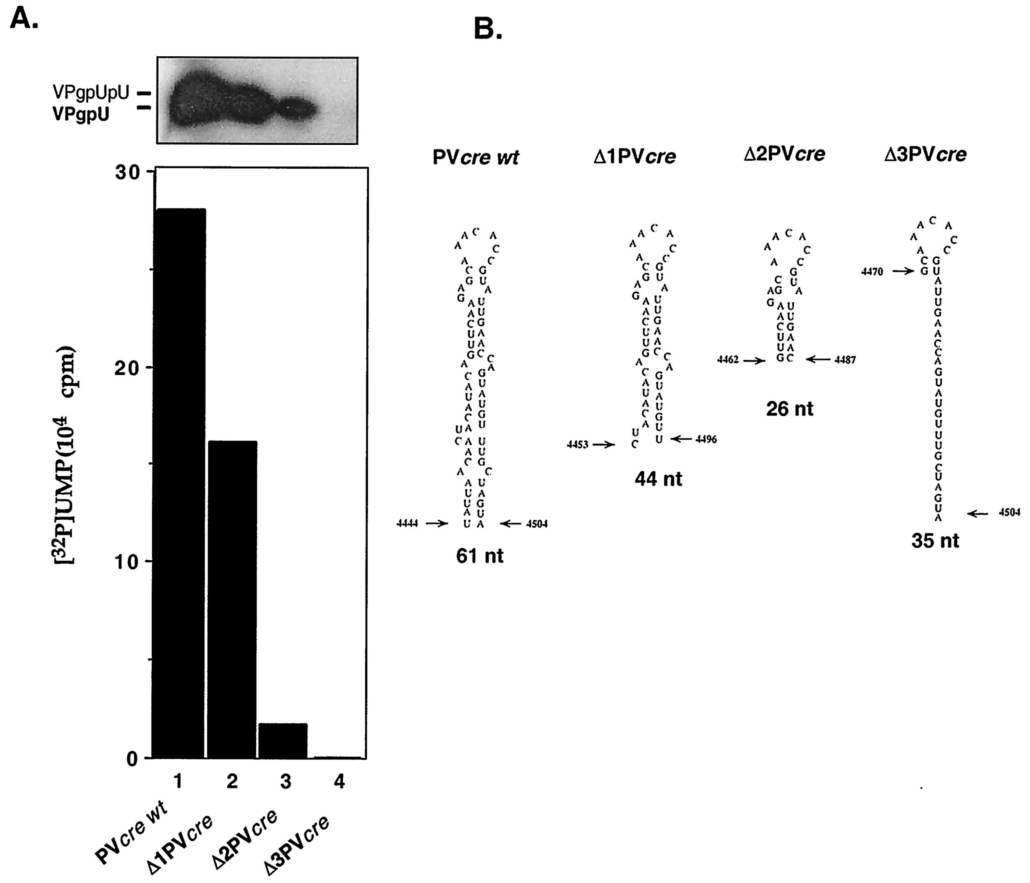

FIG. 7. In vitro uridylylation using shortened PV-*cre*(2C) RNAs as templates. (A) Effect of truncation on the ability of PV-*cre*(2C) RNA to serve as the template in VPg uridylylation. The uridylylation of VPg was measured by the standard method described in Materials and Methods. The yield of the reaction (graph) was shown by autoradiography. (B) Schematic drawing of the secondary structure of complete and truncated PV-*cre* RNAs utilized in this experiment. The first and last nucleotides as well as the length of each RNA template are indicated.

true regardless of whether the recombinant $3CD^{pro}$ is attached to a His tag at the C terminus (Fig. 8) or is free of any extra tag sequence (Fig. 9A). The formation of an RNP complex between $3CD^{pro}$ and PV-*cre*(2C) could be competed by the addition of a 200-fold excess of nonlabeled PV-*cre*(2C) RNA (Fig. 8C). Moreover, this RNP complex is similarly susceptible to competition by the addition of an unlabeled plus sense cloverleaf RNA but not by its cRNA sequence (referred to as a minus sense cloverleaf; Fig. 9B). This competition experiment supports our claim of specificity since plus strand cloverleaf RNA is known to bind $3CD^{pro}$ (4, 10, 41). As expected, a 100-fold excess of domain II RNA of the poliovirus IRES, a hairpin containing an AAACCA sequence in the loop region, did not compete in $3CD^{pro}$/PV-*cre*(2C) complex formation (data not shown).

As 3AB did not bind to PV-*cre*(2C), it also did not supershift a $3CD^{pro}$/PV-*cre*(2C) complex (data not shown). This is in contrast to the formation of a 3AB/$3CD^{pro}$/cloverleaf complex, which we have shown previously to be essential for plus strand RNA synthesis (10, 38, 39). Similarly, the cellular RNA binding protein PCBP2 can form a complex with $3CD^{pro}$ and the 5′ cloverleaf (7, 21). Just like 3AB, purified PCBP2 did not bind PV-*cre*(2C) RNA (Fig. 8A, lane 3), nor did it supershift the $3CD^{pro}$/PV-*cre*(2C) complex (data not shown). These results are consistent with our previous report showing that the addition of purified 3AB or PCBP2 had no effect on the uridylylation of VPg in the presence of $3D^{pol}$, $3CD^{pro}$, and PV-*cre*(2C) (26). It is likely therefore, that 3AB and PCBP2 do not play a direct role in VPg uridylylation.

The viral RNA polymerase $3D^{pol}$ did not bind PV-*cre*(2C) RNA under the conditions of the gel shift assay (Fig. 8A, lane 5) and was also unable to influence the formation of the $3CD^{pro}$/PV-*cre*(2C) complex (Fig. 9A) in filter binding experiments. Notably, 1 μg of $3D^{pol}$, the amount of protein normally used in uridylylation experiments, did not affect the dose-response curve resulting from the binding of increasing amounts of $3CD^{pro}$ to the PV-*cre* probe (Fig. 9A).

Components of an S10 HeLa cell extract formed one or more RNP complexes with PV-*cre*(2C), even in the presence of competitor tRNA (Fig. 8B, lane 8). Preliminary data suggested that a 50-kDa protein present in HeLa cell extracts is the major component that binds PV-*cre*(2C) (data not shown). However, early studies have indicated that the addition of an extract of uninfected HeLa cells did not stimulate the uridylylation reaction under the condition of the experiments (26). Currently we

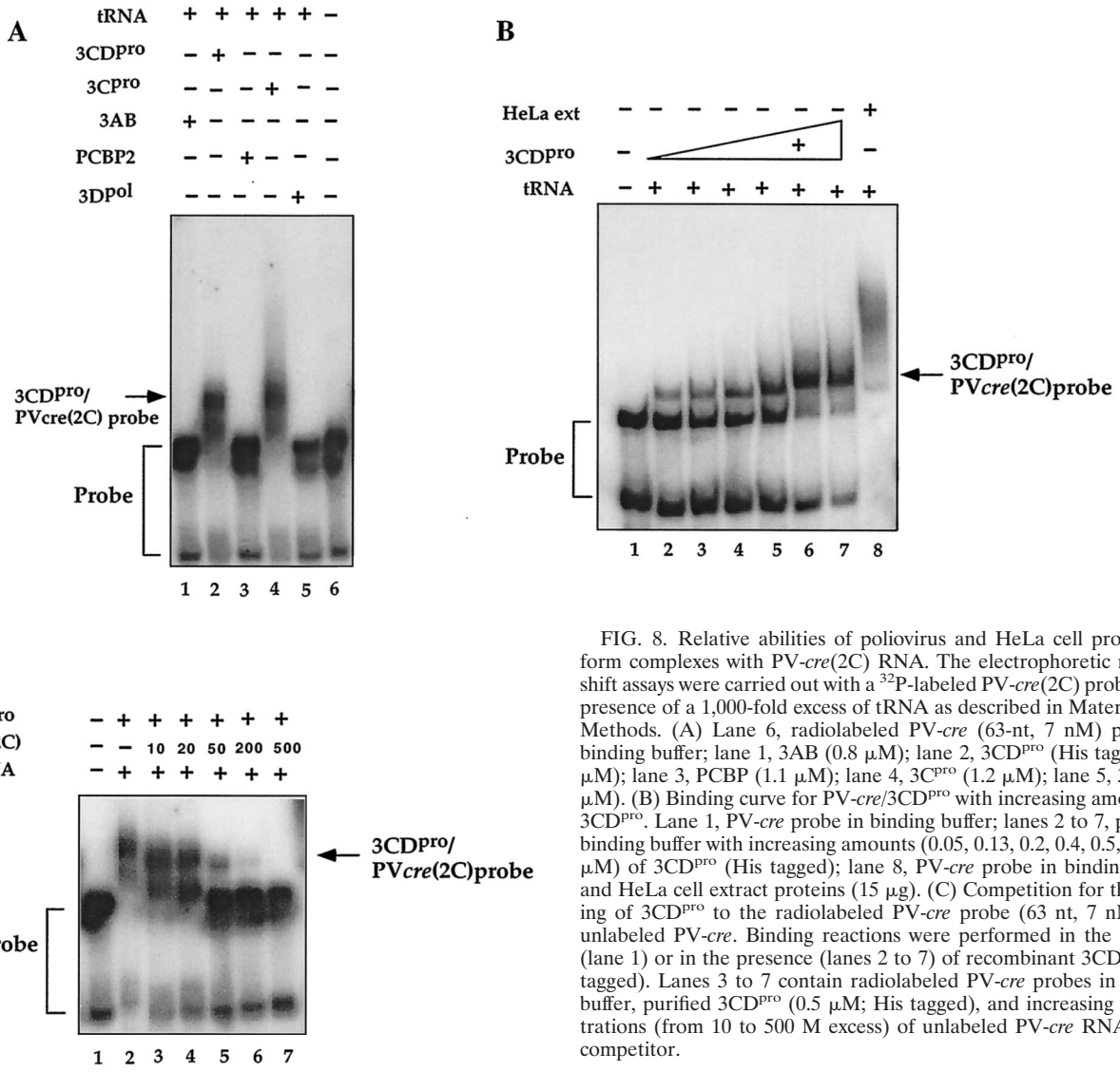

FIG. 8. Relative abilities of poliovirus and HeLa cell proteins to form complexes with PV-*cre*(2C) RNA. The electrophoretic mobility shift assays were carried out with a ^{32}P-labeled PV-*cre*(2C) probe in the presence of a 1,000-fold excess of tRNA as described in Materials and Methods. (A) Lane 6, radiolabeled PV-*cre* (63-nt, 7 nM) probe in binding buffer; lane 1, 3AB (0.8 μM); lane 2, 3CD^{pro} (His tagged, 0.5 μM); lane 3, PCBP (1.1 μM); lane 4, 3C^{pro} (1.2 μM); lane 5, 3D^{pol} (1 μM). (B) Binding curve for PV-*cre*/3CD^{pro} with increasing amounts of 3CD^{pro}. Lane 1, PV-*cre* probe in binding buffer; lanes 2 to 7, probe in binding buffer with increasing amounts (0.05, 0.13, 0.2, 0.4, 0.5, and 0.6 μM) of 3CD^{pro} (His tagged); lane 8, PV-*cre* probe in binding buffer and HeLa cell extract proteins (15 μg). (C) Competition for the binding of 3CD^{pro} to the radiolabeled PV-*cre* probe (63 nt, 7 nM) with unlabeled PV-*cre*. Binding reactions were performed in the absence (lane 1) or in the presence (lanes 2 to 7) of recombinant 3CD^{pro} (His tagged). Lanes 3 to 7 contain radiolabeled PV-*cre* probes in binding buffer, purified 3CD^{pro} (0.5 μM; His tagged), and increasing concentrations (from 10 to 500 M excess) of unlabeled PV-*cre* RNA as the competitor.

do not know the identity of the cellular protein, nor do we know its function.

To test whether mutations in the loop or stem of PV-*cre*(2C) affect the binding to 3CD^{pro}, we performed filter-binding assays with selected mutant PV-*cre* RNA probes. As shown in Fig. 9C, use of C_8A, A_9G, $C_{10}U$ $C_{11}U$, A_9U, C_8U A_9G, or A_5C loop mutant RNA or $A_{14}C$ stem mutant RNA resulted in the retention of amounts of 3CD^{pro} on the nitrocellulose membrane similar to that resulting from the use of the wt PV-*cre* probe. Interestingly, quantification of the binding of the PV-*cre* G_1U and $G_{4462}A$ $C_{4465}U$ (mut1 in reference 30) mutant RNAs revealed an 8- to 15-fold reduction in binding to 3CD^{pro}, as judged by a decreased amount of RNP complex retained on the nitrocellulose membranes. The diminution in binding of PV-*cre* G_1U and $G_{4462}A$ $C_{4465}U$ RNAs by 3CD^{pro} is in agreement with our uridylylation studies and the phenotypic properties of either the full-length viral genome ($G_{4462}A$ $C_{4465}U$) (30) or a replicon RNA (G_1U) (Fig. 3B).

DISCUSSION

Originally, the highly structured 5′ and 3′ NTR sequences of entero- and rhinovirus genomes were considered necessary and sufficient for the initiation of RNA replication (1). The discovery of internal *cre* elements, first described by McKnight and Lemon (18) for HRV14, which are also essential for viral RNA replication, came as a surprise. Similarly surprising was the subsequent observation that these elements can direct 3D^{pol}-catalyzed uridylylation of VPg, thereby providing the primer for the initiation of RNA synthesis (8, 26, 30). A suggestion that the poliovirus cloverleaf is involved in VPg uridylylation was provided in a recent report by Lyons et al. (16). This finding, together with the recent model of the circularization of the poliovirus genome prior to RNA synthesis (11), suggests that at least three RNA domains (5′-terminal cloverleaf, *cre*, and 3′-terminal poly[A]) must interact with viral and cellular polypeptides to orchestrate the initiation of minus

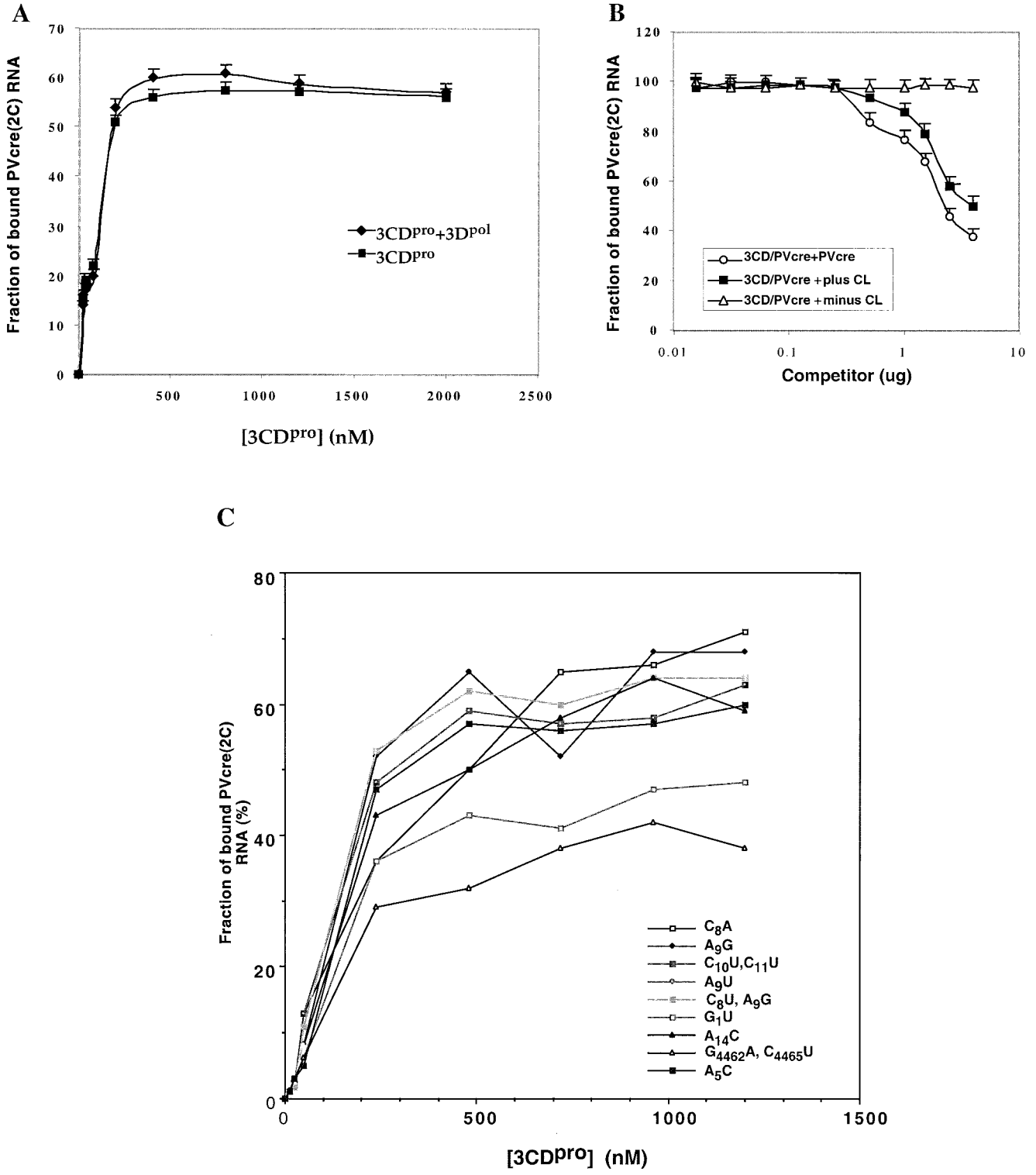

FIG. 9. Filter binding assays to assess the effect of addition of $3D^{pol}$ or competitor (mutant PV-*cre* or cloverleaf) RNAs on the binding of $3CD^{pro}$ to PV-*cre*(2C). (A) Binding reaction between PV-*cre*(2C) (63 nt, 7 nM) and $3CD^{pro}$ (0.01 to 0.8 μM, untagged) performed in the absence (squares) or in the presence (diamonds) of 1 μM $3D^{pol}$. $3CD^{pro}$ used in this experiment and that described in the panel B legend is a recombinant ($3C^{pro}$/H40A) protein that does not carry additional tag sequences (23). The filter binding data collected are shown as the means of three measurements at each data point. (B) Effect of plus and minus strand poliovirus cloverleaf and wt PV-*cre* on the binding of $3CD^{pro}$ to PV-*cre*. Competition was performed in the presence of either PV-*cre* (circles) or plus strand cloverleaf (squares) or minus strand cloverleaf (triangles) RNA competitors. Quantitative analysis of the $3CD^{pro}$/PV-*cre* complexes was carried out by using a filter-binding assay as described in Materials and Methods. (C) Comparison of the relative binding affinities of wt and mutant PV-*cre* RNAs for the site within $3CD^{pro}$ in a filter-binding assay as described in Materials and Methods.

strand synthesis. The details of these events are not yet understood.

We have focused on the *cre* elements of poliovirus, HRV14, and HRV2 to decipher structural parameters by genetic and biochemical analyses. With the exception of those of foot-and-mouth disease virus (17), all *cre* elements described so far are located in the ORFs encoding components of polyproteins (8, 9, 15, 18). Genetic analysis requires site-directed mutagenesis of the cognate PV-*cre*(2C) without destroying $2C^{ATPase}$ function, a strategy that is severely limited. Therefore, in this study, the cognate *cre* was inactivated by a single point mutation (A_5C) and a second *cre* was inserted to rescue genome replication. Since McKnight and Lemon (18) and Goodfellow et al. (9) had shown previously that HRV14-*cre* and PV3-*cre*, respectively, could be moved from their original locations, our strategy was likely to work. Indeed, the data presented here show that a second *cre* element, even if it was derived from a different picornavirus, was efficient in rescuing replication. As any genetic alteration at the second *cre* does not complicate the proper processing and functioning of viral proteins, the dual-*cre* system was suitable for genetic analyses. Remarkably, the location of the second *cre* had no detectable effect on its rescuing function, even when it mapped to the region between the cloverleaf and the IRES.

Our genetic and biochemical analyses have led to the designation of a core sequence (Fig. 2B) essential for *cre* function. A similar core sequence has been proposed very recently also by Yang et al. (40) based on an analysis of HRV14-*cre*. Mutations within the conserved 14-nt core sequence (Fig. 2) produce phenotypes that suggest that several purines within this core sequence, i.e., G_1, A_5, A_6, and A_{14}, are necessary for *cre* function. Interestingly, transition mutations in the loop ($C_{10}U$ and $C_{11}U$) that may lead to base pairing with A_5 and A_6 abolished *cre* function in uridylylation and rendered the genome nonviable even after four passages. This observation indicates that a degree of structural integrity in the core sequence is essential for its function. The preferred nucleotide in position 1 of the core is the purine G, which is highly sensitive to base pairing since a mutant carrying an $A_{14}C$ transversion reduces the luciferase signal dramatically in the dual-*cre* replicon system and nearly abolishes *cre*-dependent uridylylation of VPg.

Although PV-*cre*s with mutation in G_1 or A_{14} of the core sequence produced a reduction in *cre* function when used as a rescuer in the dual-*cre* replicon system, the role of G_1 appears to be more important than that of A_{14}. Transversions are not tolerated at the G_1 position, whereas the $A_{14}U$ mutant is still active in VPg uridylylation in vitro and in the rescue function in vivo. Initially, we were surprised about the functional activity of the $A_{14}U$ mutant since either a C or a U at nt 14 of the core sequence could base pair with G_1. However, since U_{14} has the option to base pair with A_2 and since A_2 is not essential for *cre* function (J. Yin and E. Wimmer, unpublished data), an A_2::U_{14} base pairing may not be debilitating. Perhaps the observed conservation of an A at position 14 is solely due to the fact that this A is the least favorable nucleotide to base pair with G_1.

Experiments with truncated PV-*cre* elements (Fig. 7) support our previous finding that important structural determinants for *cre* function are contained in the upper stem and loop region. Δ2 PV-*cre*(2C) RNA, consisting of only 26 nt, can still function as a template for VPg uridylylation although the template activity is greatly reduced. The artificial *cre* has even fewer virus-specific nucleotides, yet it is not only an excellent template for uridylylation in vitro but also an efficient rescue element in vivo (Fig. 3 and 4). These results suggest that the sequences contained in the middle and bottom regions of the *cre* stem might be required only for proper structural presentation of the core sequence. This conclusion is in agreement with evidence derived from mutational analyses of *cre* elements of poliovirus and HRVs (8, 9, 18, 19, 30, 40).

The flexibility by which the poliovirus genome tolerates different locations of the *cre* element is surprising. Even when placed between two highly structured entities, the cloverleaf and the IRES, nearly wt function was retained. These results suggest that sequences in the vicinity of the cognate *cre* play little if any role in *cre* function. Mason et al. (17) have recently shown that the *cre* element of foot-and-mouth disease virus, an aphthovirus, is located in the 5′-terminal region of its genome and could be moved to the 3′ NTR. This result, together with the other known locations of *cre* elements in entero-, rhino-, and cardiovirus genomes, supports the notion that *cre*-mediated uridylylation is location independent.

We have previously reported that *cre* RNAs of HRV14 and HRV2 can serve as templates in the uridylylation of poliovirus VPg in vitro in the presence of poliovirus $3D^{pol}$ and $3CD^{pro}$ (8, 26). We now show that these heterologous *cre* elements are capable also of rescuing RNA synthesis in dual-*cre* genomes of replicons in vivo. The efficiency of the rescuing ability covaries with the efficiency of in vitro uridylylation: HRV14-*cre* is far superior to HRV2-*cre* (Fig. 3A). Of the three *cre*s that we have analyzed, that of HRV2 has the smallest loop domain. Whereas this configuration must be optimal for HRV2 replication, it is suboptimal for poliovirus polypeptides such as VPg, $3D^{pol}$, and $3CD^{pro}$ that must recognize it. It appears that the poliovirus polypeptides, as well as those of HRV14, prefer a larger loop since a $U_{11}C$ mutation in HRV2-*cre* enhances significantly both the rescue function and template function in uridylylation.

Our dual-*cre* viruses showed less-than-expected differences when analyzed in one-step growth curve experiments. Compared to the results from in vitro uridylylation assays using dual-*cre* P/L replicon RNAs, the differences in viral growth kinetics in vivo are far less pronounced. The reason for this unexpected result is unknown. One possible explanation is that in infected cells VPg-pUpU is synthesized in excess of what is needed to produce progeny RNAs. Another possibility is that reversions in the mutated PV-*cre*(2C) emerge rapidly to obscure the original replication phenotype. However, we have sequenced both *cre* regions in plaque-purified dual-*cre* viruses isolated after the second passage and have found that the A_5C mutation in the $2C^{ATPase}$ locus was always retained. However, in two out of four progeny viruses that were plaque purified after two passages of PV (A_5C)/HRV2-*wt*(S) virus, we found an identical $U_{11}C$ transition in HRV2-*cre*, a mutation that enhances HRV2-*cre* function in the context of the poliovirus genome. In any event, we cannot exclude the possibility that some of the isolates after the second passage harbor second-site suppressor mutations.

Nothing has been known about the mechanism of interac-

tion between viral polypeptides and *cre* elements. Equally obscure is the possible participation of cellular polypeptides in uridylylation. For this reason, we have conducted protein binding studies using gel mobility shift and filter binding assays. We found that $3CD^{pro}$ and its cleavage product $3C^{pro}$, but not $3D^{pol}$, recognize PV-*cre*(2C) with high specificity. Other RNA binding proteins known to be involved in poliovirus RNA replication, e.g., 3AB and PCBP2, did not display affinity to *cre* under the conditions of the experiment. Available evidence suggests that it is the $3C^{pro}$ moiety of $3CD^{pol}$ that is responsible for the binding of the polypeptide to *cre* (26). Moreover, since $3C^{pro}$ can stimulate uridylylation, first reported by Pathak et al. (23) and confirmed here, $3D^{pol}$ may directly bind to an as yet undefined region in $3C^{pro}$ (23). Preliminary experiments support this hypothesis (J. Yin, E. Wimmer, and E. Rieder, unpublished results). On the other hand, no binding between $3D^{pol}$ and $3C^{pro}$ was observed in a yeast two-hybrid system (37), which may be a false-negative result.

We have not yet been able to determine those nucleotides in PV-*cre*(2C) making contact with $3CD^{pro}$ or $3C^{pro}$. Our data suggest that recognition of the RNA may involve more than 1 nt located in the upper bulge and upper terminal stem. This hypothesis is based on the observation that the G_1U ($G_{4468}U$ and $G_{4462}A$ $C_{4465}U$) mutants were less efficient not only in replication but also in the formation of the RNP complex. In contrast, all mutants with mutations in the terminal loop (including the one altering the first critical A_5C nucleotide) bind to $3CD^{pro}$ or $3C^{pro}$ with efficiencies similar to that of wt PV-*cre*. Whether the formation of an RNP complex stabilizes the configuration of *cre* or whether this event is necessary for putative structural changes in the $3C^{pro}$ moiety for $3D^{pol}$/VPg recruitment remains to be seen.

All available evidence suggests that the first step in poliovirus RNA synthesis is *cre*-dependent uridylylation of VPg by $3D^{pol}$, yielding the primer for minus strand synthesis. Because of its internal location, Paul has designated the function of the *cre* locus *ori*I (24). The observation that *cre* elements can be moved to different genome loci supports this designation. However, the mechanism by which the VPg-pUpU/3D/3CD initiation complex is subsequently moved to the 3′ terminus for the initiation of minus strand RNA synthesis remains a puzzle. It has been proposed that the initiation of minus strand synthesis requires the poliovirus genome to circularize (5, 11). As has been proposed by Paul (24) and Pathak et al. (23), we suggest that an initiation complex formed at any *ori*I locus within a circular RNA could bind to the 3-terminal poly(A) by template displacement in *cis*.

ACKNOWLEDGMENTS

We thank Anna Niewiadomska and JoAnn Mugavero for expert assistance. We thank C. E. Cameron for sharing unpublished data and for supplying recombinant non-His-tagged $3CD^{pro}$ and $3C^{pro}$-His expression vectors and proteins. Our extended gratitude goes to B. Semler for providing a PCBP-expression vector, X. Li for providing the P/L replicon plasmid, and K. Kirkergaard for providing the $3D^{pol}$ vector.

This work was supported by grant AI15122 of the National Institute of Allergy and Infectious Diseases.

REFERENCES

1. **Agol, V. I., A. V. Paul, and E. Wimmer.** 1999. Paradoxes of the replication of picornaviral genomes. Virus Res. **62:**129–147.
2. **Ambros, V., and D. Baltimore.** 1978. Protein is linked to the 5′ end of poliovirus RNA by phosphodiester linkage to tyrosine. J. Biol. Chem. **253:** 5263–5266.
3. **Andino, R., G. E. Rieckhof, P. L. Achacoso, and D. Baltimore.** 1993. Poliovirus RNA synthesis utilizes an RNP complex formed around the 5′-end of viral RNA. EMBO J. **12:**3587–3598.
4. **Andino, R., G. E. Rieckhof, and D. Baltimore.** 1990. A functional ribonucleoprotein complex forms around the 5′ end of poliovirus RNA. Cell **63:**369–380.
5. **Barton, D. J., B. J. O'Donnell, and J. B. Flanegan.** 2001. 5′ cloverleaf in poliovirus RNA is a *cis*-acting replication element required for negative-strand synthesis. EMBO J. **20:**1439–1448.
6. **Blyn, L. B., K. M. Swiderek, O. Richards, D. C. Stahl, B. L. Semler, and E. Ehrenfeld.** 1996. Poly(rC) binding protein 2 binds to stem-loop IV of the poliovirus RNA 5′ noncoding region: identification by automated liquid chromatography-tandem mass spectrometry. Proc. Natl. Acad. Sci. USA **93:**11115–11120.
7. **Gamarnik, A. V., and R. Andino.** 1997. Two functional complexes formed by KH domain containing proteins with the 5′ noncoding region of poliovirus RNA. RNA **3:**882–892.
8. **Gerber, K., E. Wimmer, and A. V. Paul.** 2001. Biochemical and genetic studies of the initiation of human rhinovirus 2 RNA replication: identification of a *cis*-replicating element in the coding sequence of $2A^{pro}$. J. Virol. **75:**10979–10990.
9. **Goodfellow, I., Y. Chaudhry, A. Richardson, J. Meredith, J. W. Almond, W. Barclay, and D. J. Evans.** 2000. Identification of a *cis*-acting replication element within the poliovirus coding region. J. Virol. **74:**4590–4600.
10. **Harris, K. S., W. Xiang, L. Alexander, W. S. Lane, A. V. Paul, and E. Wimmer.** 1994. Interaction of poliovirus polypeptide $3CD^{pro}$ with the 5′ and 3′ termini of the poliovirus genome. Identification of viral and cellular cofactors needed for efficient binding. J. Biol. Chem. **269:**27004–27014.
11. **Herold, J., and R. Andino.** 2001. Poliovirus RNA replication requires genome circularization through a protein-protein bridge. Mol. Cell **7:**581–591.
12. **Jang, S. K., H.-G. Kräusslich, M. J. H. Nicklin, G. M. Duke, A. C. Palmenberg, and E. Wimmer.** 1988. A segment of the 5′ nontranslated region of encephalomyocarditis virus RNA directs internal entry of ribosomes during in vitro translation. J. Virol. **62:**2636–2643.
13. **Lama, J., A. V. Paul, K. S. Harris, and E. Wimmer.** 1994. Properties of purified recombinant poliovirus protein 3AB as substrate for viral proteinases and as co-factor for viral polymerase $3D^{pol}$. J. Biol. Chem. **269:**66–70.
14. **Li, X., H. H. Lu, S. Mueller, and E. Wimmer.** 2001. The C-terminal residues of poliovirus proteinase $2A^{(pro)}$ are critical for viral RNA replication but not for *cis*- or *trans*-proteolytic cleavage. J. Gen. Virol. **82:**397–408.
15. **Lobert, P. E., N. Escriou, J. Ruelle, and T. Michiels.** 1999. A coding RNA sequence acts as a replication signal in cardioviruses. Proc. Natl. Acad. Sci. USA **96:**11560–11565.
16. **Lyons, T., K. E. Murray, A. W. Roberts, and D. J. Barton.** 2001. Poliovirus 5′-terminal cloverleaf RNA is required in *cis* for VPg uridylylation and the initiation of negative-strand RNA synthesis. J. Virol. **75:**10696–10708.
17. **Mason, P. W., S. V. Bezborodova, and T. M. Henry.** 2002. Identification and characterization of a *cis*-acting replication element (*cre*) adjacent to the IRES of foot-and-mouth disease virus. J. Virol. **76:**9686–9694.
18. **McKnight, K. L., and S. M. Lemon.** 1996. Capsid coding sequence is required for efficient replication of human rhinovirus 14 RNA. J. Virol. **70:** 1941–1952.
19. **McKnight, K. L., and S. M. Lemon.** 1998. The rhinovirus type 14 genome contains an internally located RNA structure that is required for viral replication. RNA **4:**1569–1584.
20. **Molla, A., A. V. Paul, and E. Wimmer.** 1991. Cell-free, de novo synthesis of poliovirus. Science **254:**1647–1651.
21. **Parsley, T. B., J. S. Towner, L. B. Blyn, E. Ehrenfeld, and B. L. Semler.** 1997. Poly (rC) binding protein 2 forms a ternary complex with the 5′-terminal sequences of poliovirus RNA and the viral 3CD proteinase. RNA **3:**1124–1134.
22. **Pata, J. D., S. C. Schultz, and K. Kirkegaard.** 1995. Functional oligomerization of poliovirus RNA-dependent RNA polymerase. RNA **1:**466–477.
23. **Pathak, H. B., S. K. Ghosh, A. W. Roberts, S. D. Sharma, J. D. Yoder, J. J. Arnold, D. W. Gohara, D. J. Barton, A. V. Paul, and C. E. Cameron.** 2002. Structure-function relationships of the RNA-dependent RNA polymerase from poliovirus ($3D^{pol}$): a surface of the primary oligomerization domain functions in capsid precursor processing and VPg uridylylation. J. Biol. Chem. **277:**31551–31562.
24. **Paul, A. V.** 2002. Possible unifying mechanism of picornavirus genome replication, p. P. 227–246. *In* B. L. Semler and E. Wimmer (ed.), Molecular biology of picornaviruses. ASM Press, Washington, D.C.
25. **Paul, A. V., X. Cao, K. S. Harris, J. Lama, and E. Wimmer.** 1994. Studies with poliovirus polymerase $3D^{pol}$. Stimulation of poly(U) synthesis *in vitro* by purified poliovirus protein 3AB. J. Biol. Chem. **269:**29173–29181.
26. **Paul, A. V., E. Rieder, D. W. Kim, J. H. van Boom, and E. Wimmer.** 2000. Identification of an RNA hairpin in poliovirus RNA that serves as the primary template in the in vitro uridylylation of VPg. J. Virol. **74:**10359–10370.
27. **Paul, A. V., J. H. van Boom, D. Filippov, and E. Wimmer.** 1998. Protein-

primed RNA synthesis by purified poliovirus RNA polymerase. Nature **393:** 280–284.
28. **Pelletier, J., and N. Sonenberg.** 1988. Internal initiation of translation of eukaryotic mRNA directed by a sequence derived from poliovirus RNA. Nature **334:**320–325.
29. **Pfister, T., and E. Wimmer.** 1999. Characterization of the nucleotide triphosphatase activity of poliovirus protein 2C reveals a mechanism by which guanidine inhibits replication of poliovirus. J. Biol. Chem. **274:**6992–7001.
30. **Rieder, E., A. V. Paul, D. W. Kim, J. H. van Boom, and E. Wimmer.** 2000. Genetic and biochemical studies of poliovirus *cis*-acting replication element *cre* in relation to VPg uridylylation. J. Virol. **74:**10371–10380.
31. **Roehl, H. H., T. B. Parsley, T. V. Ho, and B. L. Semler.** 1997. Processing of a cellular polypeptide by 3CD proteinase is required for poliovirus ribonucleoprotein complex formation. J. Virol. **71:**578–585.
32. **Rothberg, P., T. Harris, A. Nomoto, and E. Wimmer.** 1978. 0^4-(5′-Uridylyl)-tyrosine is the bond between the genome-linked protein and the RNA of poliovirus. Proc. Natl. Acad. Sci. USA **75:**4868–4872.
33. **Skern, T., W. Sommergruber, D. Blaas, P. Gruendler, F. Fraundorfer, C. H. Pieler, I. Fogy, and E. Kuechler.** 1985. Human rhinovirus 2: complete nucleotide sequence and proteolytic processing signals in the capsid protein region. Nucleic Acids Res. **13:**2111–2126.
34. **Stanway, G., P. J. Hughes, R. C. Mountford, P. D. Minor, and J. W. Almond.** 1984. The complete nucleotide sequence of a common cold virus: human rhinovirus 14. Nucleic Acids Res. **12:**7859–7875.
35. **Todd, S., J. S. Towner, D. M. Brown, and B. L. Semler.** 1997. Replication-competent picornaviruses with complete genomic RNA 3′ noncoding region deletions J. Virol. **71:**8868–8874.
36. **van der Werf, S., J. Bradley, E. Wimmer, F. W. Studier, and J. J. Dunn.** 1986. Synthesis of infectious poliovirus RNA by purified T7 RNA polymerase. Proc. Natl. Acad. Sci. USA **83:**2330–2334.
37. **Xiang, W., A. Cuconati, D. Hope, K. Kirkegaard, and E. Wimmer.** 1998. Complete protein linkage map of poliovirus P3 proteins: interaction of polymerase $3D^{pol}$ with VPg and with genetic variants of 3AB. J. Virol. **72:**6732–6741.
38. **Xiang, W., A. Cuconati, A. V. Paul, X. Cao, and E. Wimmer.** 1995. Molecular dissection of the multifunctional poliovirus RNA-binding protein 3AB. RNA **1:**892–904.
39. **Xiang, W., K. S. Harris, L. Alexander, and E. Wimmer.** 1995. Interaction between the 5′-terminal cloverleaf and $3AB/3CD^{pro}$ of poliovirus is essential for RNA replication. J. Virol. **69:**3658–3667.
40. **Yang, Y., R. Rijnbrand, K. L. McKnight, E. Wimmer, A. Paul, A. Martin, and S. M. Lemon.** 2002. Sequence requirements for viral RNA replication and VPg uridylylation directed by the internal *cis*-acting replication element (*cre*) of human rhinovirus type 14. J. Virol. **76:**7485–7494.
41. **Ypma-Wong, M.-F., P. G. Dewalt, V. H. Johnson, J. G. Lamb, and B. L. Semler.** 1988. Protein 3CD is the major poliovirus proteinase responsible for cleavage of the P1 capsid precursor. Virology **166:**265–270.